Quantum Electronics **50** (10) 895–899 (2020)

LASERS

https://doi.org/10.1070/QEL17387

Nanosecond semiconductor disk laser emitting at 496.5 nm

M.R. Butaev, V.I. Kozlovsky, Ya.K. Skasyrsky

Abstract. **An optically pumped semiconductor disk laser based on a heterostructure containing ten CdS/ZnSe coupled quantum wells with type-II band offsets is studied. The structure was grown by metalorganic vapour phase epitaxy (MOVPE) on a GaAs substrate. The peak power of the semiconductor disk laser achieved at room temperature under longitudinal pumping by a repetitively pulsed N_2 laser was 0.75 W at a wavelength of 496.5 nm, a pulse duration of 3 ns, and a pulse repetition rate of 100 Hz. The slope efficiency of the disk laser was 2.7%. The total divergence angle at a cavity length of 1.1 mm varied from 5 mrad near the lasing threshold to 15 mrad at the maximum pump power.**

Keywords: *MOVPE, semiconductor disk laser, CdS/ZnSe heterostructure, quantum wells, optical pumping.*

1. Introduction

Extensive development of semiconductor disk lasers (SDLs) is related to their ability to generate high-power radiation with a high beam quality [1–4]. Although the present-day SDLs are based mainly on III–V heterostructures emitting in the near-IR region, the possibility of using various nonlinear effects in their cavities allows them to operate in the UV [5, 6], visible [3, 4], mid-IR [7], and submillimeter [8] spectral regions. Note that the use of the third or fourth harmonics of such SDLs considerably decreases the efficiency of the laser system as a whole [5, 9].

The aim of the present work is to create optically pumped SDLs based on II–VI heterostructures with the fundamental wavelength in the blue–green spectral region (~480–560 nm). The radiation of these lasers can be converted by relatively simple intracavity frequency doubling to the mid-UV region (~240–280 nm), which is most popular for some applications. As active media for these lasers, it is necessary to use resonant periodic gain structures of wide-gap compounds.

Radiation in the blue–green spectral range can be obtained using InGaN/GaN heterostructures and well-studied A_2B_6 heterostructures, such as ZnCdSe/ZnSSe and ZnSe/ZnMgSSe. The use of InGaN/GaN heterostructures is hardly possible at present because it is difficult to separate this heterostructure from the growth substrate (usually from sapphire) and transfer it to another transparent substrate with a high thermal conductivity, as well as to form an integrated Bragg mirror.

It is believed that the aforementioned II–VI heterostructures cannot be reliably used for laser applications because the problem of degradation of laser diodes based on these heterostructures is not yet solved [10–12]. To degradation factors, apart from those typical for injection lasers (necessity of formation p–n junction and reliable contacts), one assigns insufficiently strong chemical bonds of the second-group metal atoms with selenium and internal elastic stresses in quantum wells (QWs) [10, 13, 14]. It is obvious that only the latter degradation factors can be important for optically pumped lasers.

In [15, 16], we studied the possibility of using the ZnCdS/ZnSSe type-II heterostructure in microcavity semiconductor lasers with electron-beam pumping. It was suggested that these heterostructures, in contrast to the previously studied Zn(Cd)Se/Zn(Mg)SSe heterostructures [10, 17], are less susceptible to solid-phase diffusion at epitaxial growth temperatures and at intense excitation due to the more stable sulphide chemical bonds in QWs.

We have recently reported on lasing in a heterostructure with ten CdS/ZnSe QWs in a microcavity laser optically pumped by a repetitively pulsed N_2 laser [18]. The microcavity was formed by dielectric mirrors deposited on the surfaces of the 1.2-μm-thick heterostructure. The excited region diameter exceeded 500 μm. This led to simultaneous excitation of several tens of coherently independent lasers within the excited region with a total divergence angle of about 10°. In addition, due to a strong influence of amplified spontaneous emission in the direction perpendicular to the cavity axis, the laser efficiency did not exceed 0.3%.

In the present work, we report on lasing in a similar structure but with the use of an external feedback mirror, which allowed us to develop an optically pumped blue–green SDL for the first time.

2. Experiment

The CdS/ZnSe nanoheterostructures were grown by metalorganic vapour-phase epitaxy (MOVPE) in a hydrogen flow at atmospheric pressure in a quartz reactor. As initial compounds for the growth of structures, we used dimethyl selenide $(CH_3)_2Se$, dimethyl cadmium $(CH_3)_2Cd$, diethyl sulfide $(C_2H_5)_2S$, and diethyl zinc $(C_2H_5)_2Zn$. The structures

M.R. Butaev, V.I. Kozlovsky Lebedev Physical Institute, Russian Academy of Sciences, Leninsky prosp. 53, 119991 Moscow, Russia; National Research Nuclear University MEPhI, Kashirskoe sh. 31, 115409 Moscow, Russia;
e-mail: mbutayev@mail.ru; vikoz@sci.lebedev.ru;
Ya.K. Skasyrsky Lebedev Physical Institute, Russian Academy of Sciences, Leninsky prosp. 53, 119991 Moscow, Russia

Received 22 June 2020
Kvantovaya Elektronika **50** (10) 895–899 (2020)
Translated by M.N. Basieva

were grown on GaAs substrates disoriented by 10° from the (001) to the (111) A plane. The substrate temperature was 440 °C. The thicknesses of layers were controlled during growth by measuring reflection of the 650-nm laser diode beam focused on the growth substrate into a spot 2 mm in diameter.

The scheme of the studied heterostructure is shown in Fig. 1a. Since the CdS/ZnSe heterojunction has type II band offsets, we used in this work coupled QWs to increase the overlap integral between the electron and hole wave functions. Thus, the QW consisted of five sequentially grown layers, namely, ZnSe (4 nm), CdS (2 nm), ZnSe (2 nm), CdS (2 nm), and ZnSe (4 nm), between broad (86 nm) ZnSSe barrier layers. The structure period was ~100 nm, which should correspond to half the wavelength of laser radiation inside the structure. The first layer on the substrate was the ZnSSe buffer layer 193 nm thick, and the last ZnSSe layer had a thickness of 93 nm. These are the thicknesses at the optical control point. However, the thicknesses of layers could smoothly vary over the structure surface due to inhomogeneity of the hydrogen flow with initial components in the reactor.

The quantum well had the W configuration, which was previously used in lasers based on III–V type-II heterostructures [19]. In this case, the ZnSe layers form shallow energy wells for nonequilibrium holes, while the CdS layers form energy wells for nonequilibrium electrons. Elastic compression was partially compensated by tensile stresses in ZnSSe barrier layers, in which the sulphur concentration was about 10%. The emission spectrum of the structure was studied under pumping by an electron beam with an energy of 10 or 30 keV, a current of 4 μA, and an excitation spot diameter of 1 mm.

To fabricate an active laser element (Fig. 1b), a dielectric mirror consisting of 11 HfO_2–SiO_2 layer pairs was deposited on the structure heated to 200°C. The transmission spectrum of this mirror (mirror 1) calculated based on the measured transmission spectrum of the mirror on the control quartz substrate is presented in Fig. 2. The structure was glued with this mirror to the 5-mm-thick sapphire substrate using EPOTEK-301 optical epoxy. The thickness of the mirror coating and the glue layer considerably exceeded the thickness of the structure, which may cause additional elastic stresses in the structure.

Then, the GaAs growth substrate was removed first by grinding and then by selective chemical etching, and the single-layer Al_2O_3 antireflection coating, which decreased the coefficient of reflection from the structure surface to a level below 0.5%, was deposited on the free surface of the structure

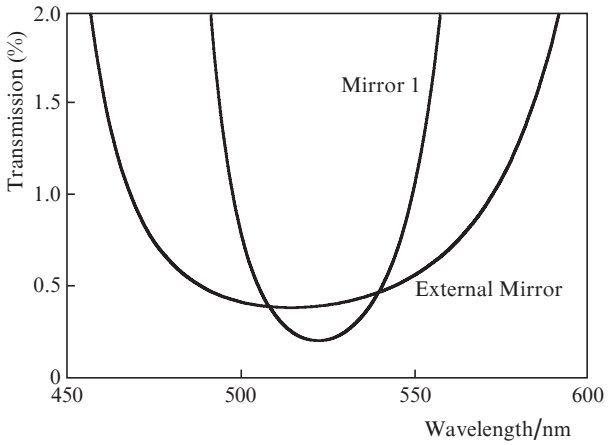

Figure 2. Transmission spectra of the mirror on the structure and the external mirror.

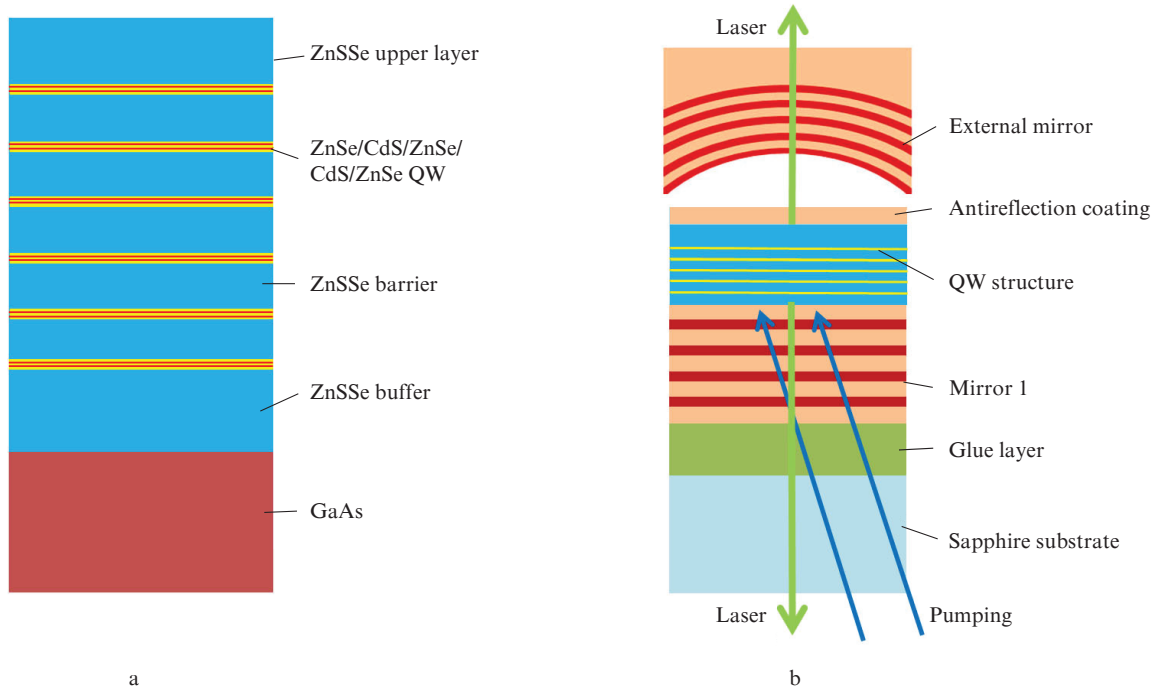

Figure 1. Schematic of (a) the initial structure and (b) the active element with the external mirror.

without heating. As the external dielectric mirror, we used a plano-concave glass substrate (radius of curvature 15 mm) with dielectric coating consisting of ZnS–Na_3AlF_6 layer pairs (Fig. 1b). The transmission spectrum of this mirror is also shown in Fig. 2. One can see that, in the wavelength range 496–497 nm, i.e., in the range of lasing, mirror 1 transmits about 1.2% and the transmission of the external mirror is 0.45%. The total outcoupling losses are 1.65% per cavity roundtrip.

The structure was longitudinally excited through the sapphire substrate by radiation of an LGI-503 nitrogen laser (λ = 337 nm) attenuated by reflection from a quartz wedge (R = 0.045). The pump pulse repetition rate was 100 Hz. The pump energy fraction reflected from the active element was 15% of the incident energy, and the pump pulse energy fraction passed through the active element did not exceed 1%. The glue layer was transparent at the pump wavelength. The generated radiation was coupled out through both the sapphire substrate (73%) and the external mirror. The pump and laser pulse shapes and peak powers were measured by a calibrated coaxial photoelectric detector FEK-22. As a filter for laser radiation, we used 10-mm-thick TF-5 glass, which completely cut off the pump radiation. The N_2 laser radiation was focused by a lens with a focal length of 150 mm into a spot 100 μm in diameter. The laser spectrum was recorded by an MDR-4 monochromator equipped with a linear CCD array.

3. Experimental results and discussion

Figure 3 shows the oscillograms of pump and laser pulses at an incident peak pump power of 62 W. One can see that the laser pulse appears with a delay of about 4 ns from the beginning of the pump pulse and the laser pulse duration at half maximum slightly exceeds 3 ns.

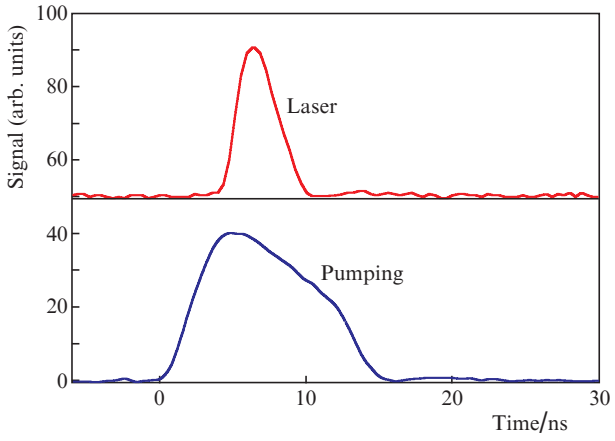

Figure 3. Oscillograms of pump and laser pulses.

The dependence of the laser peak power on the pump peak power incident on the active element in shown in Fig. 4 for a cavity length of 1.1 mm (the laser peak power is determined as the total power coupled out through the sapphire substrate and the external mirror). The lasing threshold was 35 W, which corresponds to a peak pump intensity of 445 kW cm^{-2}. The laser slope efficiency was 2.7%.

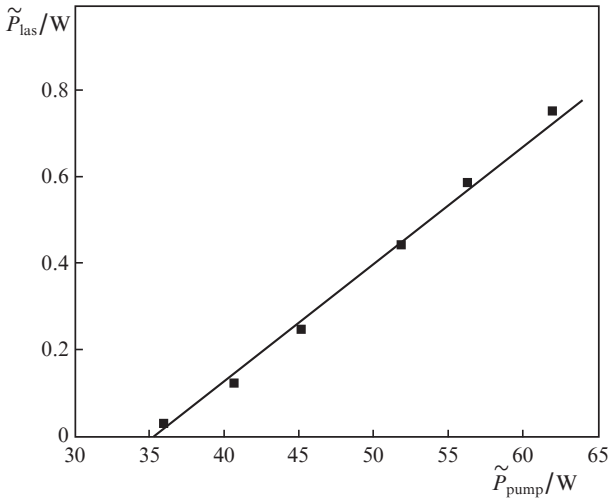

Figure 4. Dependence of the peak laser pulse power on the incident peak pump power.

Note that the obtained lasing threshold approximately corresponds to the thresholds of pulsed SDLs based on other materials. In particular, the threshold pump intensity for SDLs based on the InGaN/GaN structure (393 nm) excited by nanosecond N_2 laser pulses was 700 kW cm^{-2} [20], while the corresponding intensity for a pulsed SDL based on the AlGaInAs/InP structure (1570 nm) at a pump wavelength of 1064 nm was approximately 250 kW cm^{-2} [21], which is equivalent to 750 kW cm^{-2} for the wavelength of 337 nm. The threshold pump intensity for an SDL based on the GaInP/AlGaInP structure (625 nm) in the case of pumping by the second harmonic of a Nd:YAG laser (532 nm) was 760 kW cm^{-2} [22]. Lasing thresholds in the case of cw excitation are usually an order of magnitude lower than in the case of pulsed pumping [23]. This allows us to hope to obtain cw lasing in the studied structures.

The slope efficiency of lasers depends on the pump pulse duration and the photon lifetime in the cavity. The slope efficiency at pulse durations of ~100 ns and a cavity length of 10 mm is about 10%–15% [21]. In our experiment, the pump pulse duration was 8–10 ns, the cavity length was 1 mm, and the useful outcoupling losses per cavity roundtrip were 1.65%. The closest experimental conditions were used in work [20] devoted to the study of an SDL based on the InGaN/GaN structure, the authors of which achieved a slope efficiency of 3.5% at a pump pulse duration of 2.7 ns, a cavity length of 2 mm, and mirror losses of 2.6% per cavity roundtrip. Taking into account the difference between the energies of generated photons (496.5 nm in the present work and 393 nm in [20]), we find that the quantum efficiencies of both lasers are almost identical. Nevertheless, the obtained low pumping efficiency can be explained not only by the pulsed pumping regime, but also by high internal losses, nonuniform pump distribution over the structure depth, and enhanced spontaneous emission propagating along the structure.

Figure 5a shows the cathodoluminescence spectrum of the initial grown structure at room temperature and a low electron-beam pumping level. At an electron energy of 30 keV, the structure was pumped uniformly over the depth, while pumping with an electron energy of 10 keV excited only the two upper QWs. With increasing electron energy,

the QW emission line slightly broadens and its peak shifts from 510 to 508 nm. This is probably related to a slight change in the thickness of layers in the process of growth. The arrow in Fig. 5a indicates the wavelength of the spectral peak of the laser based on the considered structure. The short-wavelength shift of the laser line with respect to the cathodoluminescence peak is typical for lasers based on type-II heterostructures. The spectrum at an energy of 10 keV clearly shows the luminescence line of ZnSSe barrier layers. The position of this line maximum at 450 nm testifies that the sulphur concentration in the barrier layers is about 10%.

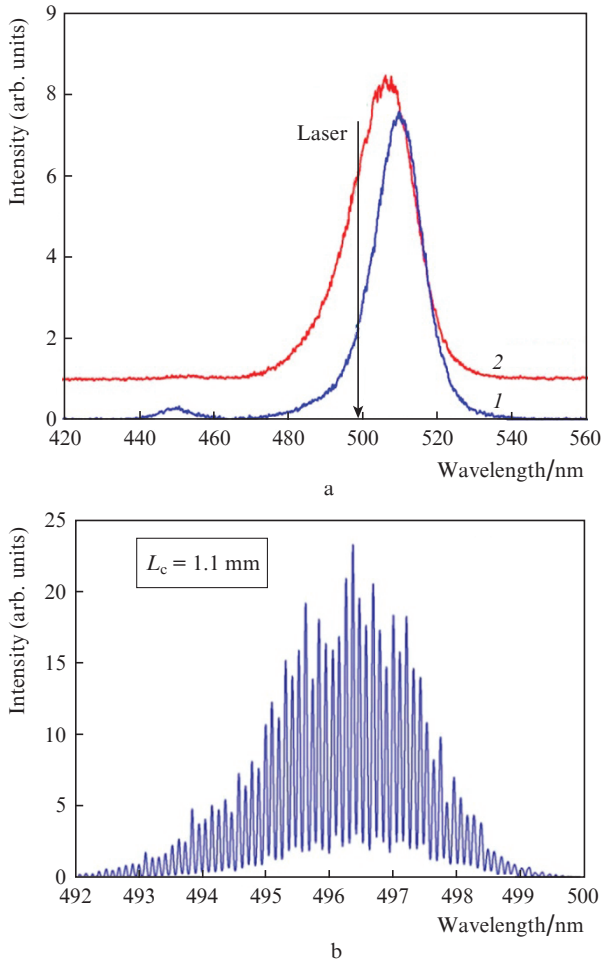

Figure 5. (a) Cathodoluminescence spectra of the initial structure at electron energies of (1) 10 and (2) 30 keV and a current of 4 μA and (b) laser spectrum at cavity length L_c = 1.1 mm.

The laser spectrum at a cavity length of ~1.1 mm is shown in Fig. 5b. It consists of many thin lines corresponding to longitudinal modes of the cavity with this length. The mode spacing makes it possible to control the cavity length with an accuracy of 0.1 mm. The minimum cavity length in our experiment was 0.9 mm, because the centre of the mirror with a curvature of 15 mm and a diameter of 10 mm cannot be closer to the plane sapphire substrate 20 mm in diameter carrying the structure. The laser characteristics deteriorated with increasing cavity length, and we failed to obtain lasing at a cavity length exceeding 3 mm. A similar dependence was observed in [20] studying an SDL based on the InGaN/GaN structure. This is related to the pulsed regime of pumping of a high-Q cavity, when the pump pulse duration is comparable with the photon lifetime in the cavity.

Figure 6 presents a typical directivity pattern of laser radiation at a slight excess of the pump power over the lasing threshold and a cavity length of 1.1 mm. This pattern corresponds to operation in the single TEM_{00} transverse mode with a total divergence angle of ~5 mrad. The calculated waist diameter of the fundamental cavity mode $2\omega_0$ is 35 μm. The total Gaussian beam divergence angle estimated by the formula $\theta = \lambda/(\pi 2\omega_0)$ is 4.5 mrad, which well corresponds to the measured value. At the maximum excess over the lasing threshold, the directivity pattern broadens approximately by three times due to excitation of several transverse modes because the size of the pumped region exceeds the fundamental mode size.

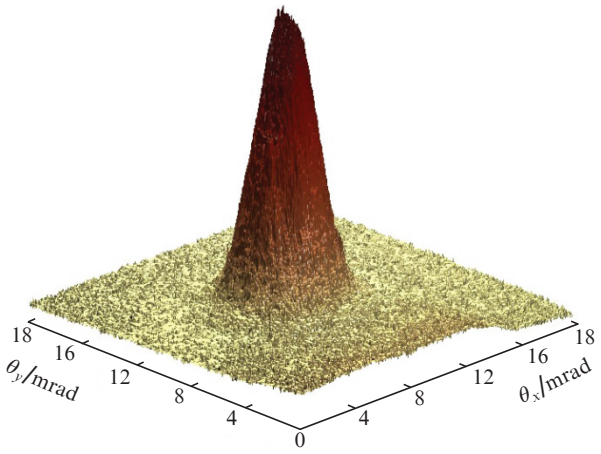

Figure 6. Far-field laser beam divergence pattern.

4. Conclusions

An optically pumped semiconductor disk laser with the fundamental wavelength in the green spectral region is developed for the first time. The laser is based on a new type-II heterostructure with ten CdS/ZnSe coupled W-shaped QWs. Laser pulses at a wavelength of 496.5 nm with a peak power of 0.75 W, a pulse duration of 3 ns, and a repetition rate of 100 Hz are obtained under longitudinal pumping by a pulsed N_2 laser. We relate the relatively low slope efficiency (2.7%) and the high lasing threshold (445 kW cm^{-2}) to nonuniform excitation of QWs over the structure depth, high quantum defect, pulsed excitation regime, and enhanced spontaneous emission propagating along the structure. Estimation of the contribution of these factors will be the subject of further investigations. The obtained results testify that, despite the type-II band offset, the studied heterostructure is promising for optically pumped blue–green semiconductor disk lasers.

Acknowledgements. This work was supported by the Russian Foundation for Basic Research (Grant No. 20-32-90022) and the Competitiveness Enhancement Programme of the National Research Nuclear University MEPhI (Grant No. 02.a03.21.0005).

References

1. Kuznetsov M., Hakimi F., Sprague R., Mooradian A. *IEEE Photonics Technol. Lett*., **9**, 1063 (1997).
2. Tropper A.C., Hoogland S. *Prog. Quantum Electron*., **30**, 1 (2006).
3. Okhotnikov O.G. *Semiconductor Disk Lasers: Physics and Technology* (Weinheim: Wiley-VCH, 2010).
4. Hastie J.E., Calvez S., Dawson M.D., in *Semiconductor Lasers* (Woodhead Publishing Limited, 2013) Vol. 9, p. 341.
5. Shu Qi-Ze, Caprara A.L., Berger J.D., Anthon D.W., Jerman H. Spinelli L. *Proc. SPIE*, **7193**, 719319 (2009).
6. Rodríguez-García J.M., Paboeuf D., Hastie J.E. *IEEE J. Sel. Top. Quantum Electron*., **23** (6), 5100608 (2017).
7. Stothard D.J.M., Hopkins J-M., Burns D., Dunn M.H. *Opt. Express*, **17** (13), 10648 (2009).
8. Scheller M., Yarborough J.M., Moloney J.V., Fallahi M., Koch M., Koch S.W. *Opt. Express*, **18** (26), 27112 (2010).
9. Kaneda Y., Wanga T.-L., Yarborougha J.M., Fallahia M., Moloneya J.V., Yoshimurab M., Morib Y., Sasaki T. *Proc. SPIE*, **7193**, 719318 (2009).
10. Ivanov S.V., Sorokin S.V., Sedova I.V., in *Molecular Beam Epitaxy* (Elsevier Inc., 2018) Vol. 25, p. 571.
11. Haase M.A., Qiu J., DePuydt J.M., Cheng H. *Appl. Phys. Lett*., **59** (11), 1272 (1991).
12. Kato E., Noguchi H., Nagai M., Okuyama H., Kijima S., Ishibashi A. *Electron. Lett*., **34** (3), 282 (1998).
13. Waag A., Litz Th., Fischer F., Lugauer H.-J., Baron T., Schüll K., Zehnder U., Gerhard T., Lunz U., Keim M., Reuscher G., Landwehr G. *J. Crystal Growth*, **184–185**, 1 (1998).
14. Law K.-K., Baude P.F., Miller T.J., Haase M.A., Haugen G.M., Smekalin K. *Electron. Lett*., **32** (4), 345 (1996).
15. Kozlovsky V.I., Sannikov D.A., Sviridov D.E. *Bull. Lebedev Phys. Inst*., **35** (2), 35 (2008) [*Kratk. Soobshch. Fiz. FIAN*, **2**, 4 (2008)].
16. Butaev M.R., Kozlovsky V.I., Sannikov D.A., Skasyrsky Y.K. *J. Phys. Conf. Ser*., **1439**, 012017 (2020).
17. Kozlovsky V.I., Kuznetsov P.I., Sviridov D.E., Yakusheva G.G. *Quantum Electron*., **42** (7), 583 (2012) [*Kvantovaya Elektron*., **42** (7), 583 (2012)].
18. Butaev M.R., Kozlovsky V.I., Skasyrsky Ya.K. *Quantum Electron*., **50** (7), 683 (2020) [*Kvantovaya Elektron*., **50** (7), 683 (2020)].
19. Möller C., Fuchs C., Berger C., Ruiz Perez A., Koch M., Hader J., Moloney J.V., Koch S.W., Stolz W. *Appl. Phys. Lett*., **108**, 071102 (2016).
20. Debusmann R., Dhidah N., Hoffmann V., Weixelbaum L., Brauch U., Graf T., Weyers M., Kneissl M. *IEEE Photonics Technol. Lett*., **22** (9), 652 (2010).
21. Huang S.C., Chang H.L., Su K.W., Li A., Liu S.C., Chen Y.F., Huang K.F. *Appl. Phys. B*, **94**, 483 (2009).
22. Kozlovsky V.I., Lavrushin B.M., Skasyrsky Ya.K., Tiberi M.D. *Quantum Electron*., **39** (8), 731 (2009) [*Kvantovaya Elektron*., **39** (8), 731 (2009)].
23. Hempler N., Hopkins J.-M., Kemp A.J., Schulz N., Rattunde M., Wagner J., Dawson M.D., Burns D. *Opt. Express*, **15** (6), 3247 (2007).